SLAC-PUB-10257
December 2003

Semileptonic B Decays at *BABAR*

Ivo Gough Eschrich

Imperial College, London SW7 2BW, U.K.
ivo@slac.stanford.edu

For the *BABAR* Collaboration

Abstract

Inclusive analyses of $\mathcal{B}(B^{+,0} \to Xe\nu)$ tagged with hadronic B-decays, $\mathcal{B}(B \to Xe\nu)$ tagged with leptons, and $\mathcal{B}(B \to X_u e\nu)$ at the kinematic endpoint are discussed. Preliminary results for the respective branching fractions and $|V_{cb}|$ and $|V_{ub}|$ are given.

Presented at Beauty 2002:
8th International Conference on B Physics at Hadron Machines,
Santiago de Compostela, Spain, 6/17/2002 - 6/21/2002

Stanford Linear Accelerator Center, Stanford University, Stanford, CA 94309
Work supported in part by the Department of Energy contract DE-AC03-76SF00515.

1 Introduction

Due to their simplicity, semileptonic decays present an excellent opportunity for the study of electroweak and strong interactions. In particular, inclusive measurements provide a straightforward, yet model dependent method to measure the coupling to the charged weak current in terms of the CKM matrix elements $|V_{cb}|$ and $|V_{ub}|$. In the standard model, semileptonic decays arise only from spectator diagrams and therefore studies of such decays illucidate the role of these diagrams in weak decays of heavy quarks. From the experimental point of view, such studies rely strongly on the identification of leptons. The *BABAR* detector [1] at the SLAC *B*-Factory is capable of separating leptons, especially electrons, from hadrons with a very low misidentification rate while retaining a high selection efficiency. It is an ideal tool for inclusive studies of semileptonic decays.

1.1 General strategy.

We report here on three different measurements of inclusive semileptonic branching fractions. In all of them the kinematic selection of the reconstructed decay candidates is based on the energy difference $\Delta E = E^*_B - E^*_{beam}$ and the energy substituted mass $m_{ES} = (E^{*2}_{beam} - p^{*2}_B)^{-1/2}$. They employ different ways to enhance the $B\bar{B}$ event sample — either the flavor of one B meson is tagged by a full reconstruction of its hadronic decay (section 2), or it is tagged by a high-momentum electron from a semileptonic decay (section 3), or the event sample is limited to a unique kinematic region by cutting on the electron momentum (section 4). Among the decays of the second B meson in the event, semileptonic decays are selected by identifying an electron. The flavor of the tagged B meson and the charge of this electron are used to seperate prompt ("right-sign") from cascade ("wrong-sign") decays:

$$\bar{B}^0/B^-\text{as tag:} \begin{cases} B^{0/+} \to X_{\bar{c},\bar{u}} e^+ \nu_e & \text{prompt electron ("right-sign")} \\ B^{0/+} \to X_{\bar{c}} Y, \quad X_{\bar{c}} \to Y' e^- \bar{\nu}_e & \text{cascade electron ("wrong-sign")} \end{cases}$$

In absence of other backgrounds (see below), the number of prompt electrons is identical to the number of right-sign candidates for charged B mesons. For neutral B mesons, prompt electrons can also occur in the wrong-sign sample due to $B^0\bar{B}^0$ mixing. Their contribution is given by the mixing parameter χ_0, which is precisely measured. The semileptonic branching fraction $\mathcal{B}(B \to Xe\nu)$ is calculated from the number of prompt electrons (N_{prompt}), the number of tagged B mesons (N_{tag}), and the relative efficiency for detecting a tagged event with and without a signal electron (ε_{evt}):

$$\mathcal{B}(B \to Xe\nu) = \frac{N_{prompt}}{\varepsilon_{evt} N_{tag}}$$

1.2 Electron identification.

Electrons are identfied using information from the Electromagnetic Calorimeter (EMC), the Drift Chamber (DCH), and the Cerenkov Detector (DIRC). The selection is performed either

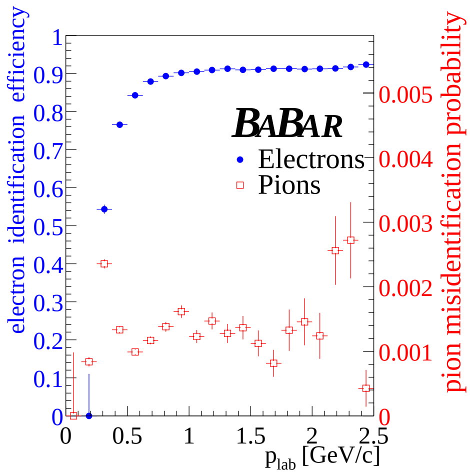

Figure 1: Efficiency and fake rates of cut-based electron identification for tracks within the EMC acceptance.

by applying subsequent cuts on the measurements from these subsystems, or by a likelihood based algorithm. Both selectors achieve more than 90% efficiency over a wide momentum range above 0.5 GeV/c while maintaining a pion fake rate well below 0.3%. As an example the cut-based selector's performance is shown in Fig. 1.

1.3 Common backgrounds.

Electrons originating from processes producing $e^- \ e^+$ pairs contribute to both right- and wrong-sign samples. Such processes are photon conversions, π^0 Dalitz decays, and J/ψ decays. They are suppressed using vertex and invariant mass cuts. We correct the observed number of such background electrons for the efficiencies of these cuts, which are determined using a full detector simulation.

Misidentified hadrons form another source of background tracks. Hadron fake rates are determined from pure samples of positive and negative pions, kaons, and protons which are selected kinematically from the decays $K_S^0 \to \pi^+\pi^-$, $D^* \to D\pi$, $D \to K\pi$ and $\Lambda \to p\pi$. Together with the relative fraction of each species in tagged events, which we determine from Monte Carlo, we estimate the momentum spectrum of this background.

We also have to consider cascade decays from the signal B meson which produce right-sign electrons in unmixed and wrong-sign electrons in mixed events:

- Semileptonic decay of a D_s^+ meson from $c\bar{c}s$ production:
  $B \to D_s^{(*)}\bar{D}$, $D_s^+ \to X'e^+\nu_e$
- Semileptonic decay of a D meson from $c\bar{c}s$ production:
  $B \to D^{(*)}\bar{D}^{(*)}K$, $D \to X'e^+\nu_e$
- Semileptonic decays with a τ lepton:
  $B \to \tau^+\nu_\tau$, $\tau^+ \to e^+\nu_e\bar{\nu}_\tau$ or $\tau^+ \to e^+\nu_e\bar{\nu}_\tau$

We determine these background spectra from Monte Carlo, where the involved branching ratios are taken from the latest measurements.

Finally, we correct for electrons in mistagged events. In the analysis using fully reconstructed B tags, these originate from combinatorial background and $B^0 \leftrightarrow B^+$ cross feed. For the analysis based on lepton tags, these are mainly due to high-momentum electrons from secondary charm decays.

2 Inclusive $\mathcal{B}(B \to Xe\nu)$ tagged with hadronic B-decays

This measurement is based on 20.6 fb^{-1} of *BABAR* data recorded in 1999 and 2000. We reconstruct the following hadronic B decays: $B \to D^{(*)}\pi$, $D^{(*)}\rho$, D^*a_1, $J/\psi K^{(*)}$, and $\psi(2S)K^{(*)}$. We reduce non-resonant background by requiring the second Fox-Wolfram moment to be smaller than 0.5. In addition, at least one more track must be present besides those assigned to the hadronic decay. The cut-based electron selector (section 1.2) has to identify at least one electron with more than 0.5 GeV/c laboratory momentum in the fiducial volume.

For charged B mesons, the number of right-sign electrons N^+_{right} is identical with the number N^+_{prompt} of prompt decays, while for decays of neutral B mesons it includes a fraction of the cascade electrons N_{casc} due to $B^0\bar{B}^0$ mixing described by the mixing parameter χ_0:

$$N^0_{right} = (1-\chi_0)N^0_{prompt} + \chi_0 N^0_{casc}$$
$$N^0_{wrong} = \chi_0 N^0_{prompt} + (1-\chi_0)N^0_{casc}$$

Source	$\Delta x/x$ [%]	$\Delta\mathcal{B}/\mathcal{B}$ [%] $(B^\pm \to X\ell\nu)$	$\Delta\mathcal{B}/\mathcal{B}$ [%] $(B^0/\bar{B}^0 \to X\ell\nu)$
Analysis efficiency	1.3 - 2.5	$\pm$ 1.3	$\pm$ 2.5
Cross-feed	2.0	$\pm$ 2.0	$\pm$ 2.0
Mixing $\Delta\chi_0$	5.2		$\pm$ 0.8
Tracking efficiency	1.5	$\pm$ 1.5	$\pm$ 1.5
Extrapolation	10	$\pm$ 1.8	$\pm$ 1.8
Physics BG		$\pm$ 1.6	$\pm$ 1.7
Electron ID	1.7	$\pm$ 1.8	$\pm$ 1.8
Hadron fakes	50	$\pm$ 1.6	$\pm$ 1.4
Pair BG	15	$\pm$ 0.18	$\pm$ 0.17
Total		$\pm$ 4.5	$\pm$ 5.0

Table 1: Systematics of $\mathcal{B}(B^{+,0} \to X_c e\nu)$ tagged with hadronic B-decays.

Therefore we can determine the prompt and cascade electron momentum spectra from the spectra of right-sign and wrong-sign electrons (Fig. 2). Extrapolation to $p = 0$ and applying acceptance corrections leads to $N^+_{prompt} = 674 \pm 34_{(stat)}$ and $N^0_{prompt} = 597 \pm 38_{(stat)}$ prompt

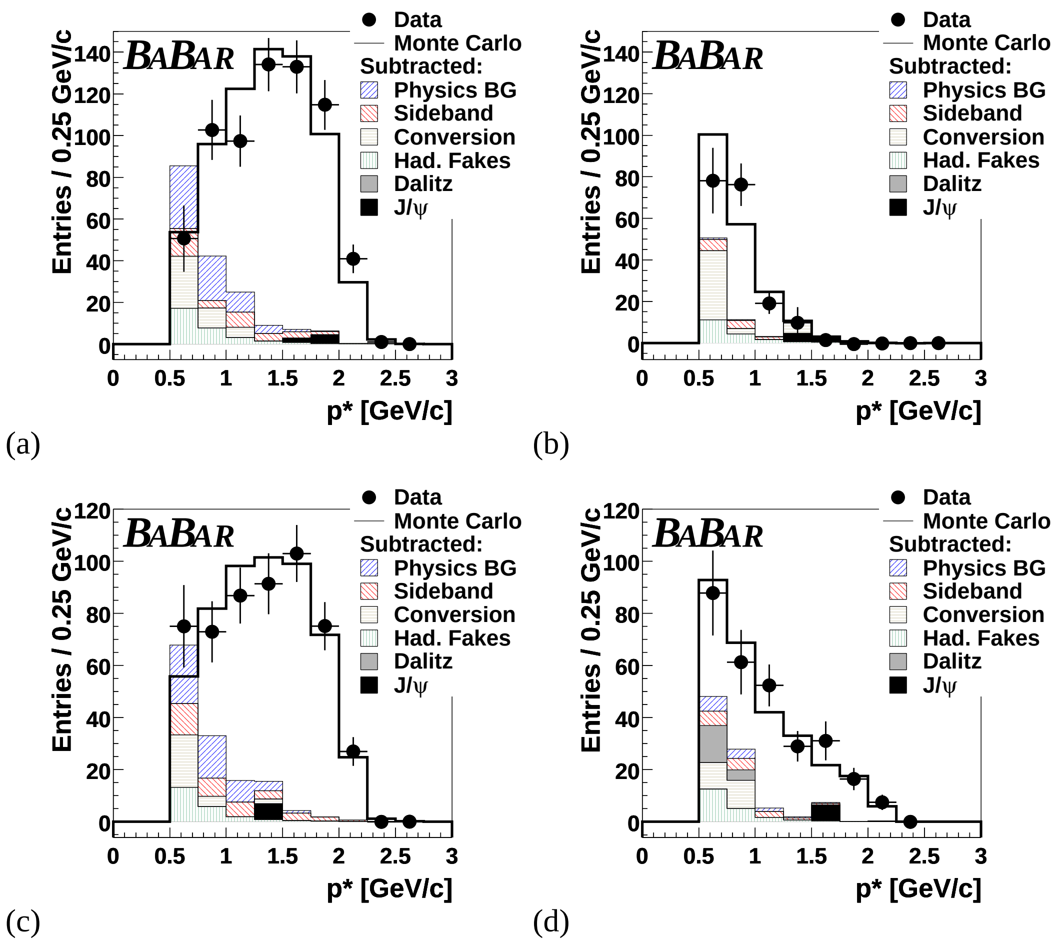

Figure 2: Momentum spectra for right-sign (a,c) and wrong-sign(b,d) electrons in events tagged with fully reconstructed $B^0/\bar{B}^0$ (a,b) and $B^{\pm}$ (c,d) decays.

electrons for charged and neutral B mesons, respectively (Figure 3). This preliminary result translates into the semileptonic branching fractions

$$
\begin{aligned}
\mathcal{B}(B^{\pm} \to X\ell\nu) =& (10.3 \pm 0.6_{(stat)} \pm 0.5_{(syst)})\% \\
\mathcal{B}(B^0/\bar{B}^0 \to X\ell\nu) =& (10.4 \pm 0.8_{(stat)} \pm 0.5_{(syst)})\% \\
\mathcal{B}(B \to X\ell\nu) =& (10.4 \pm 0.5_{(stat)} \pm 0.4_{(syst)})\% \\
\mathcal{B}(B^{\pm} \to X\ell\nu)/\mathcal{B}(B^0/\bar{B}^0 \to X\ell\nu) =& 0.99 \pm 0.10_{(stat)} \pm 0.04_{(syst)}
\end{aligned}
$$

Table 1 lists the systematic errors for this measurement.

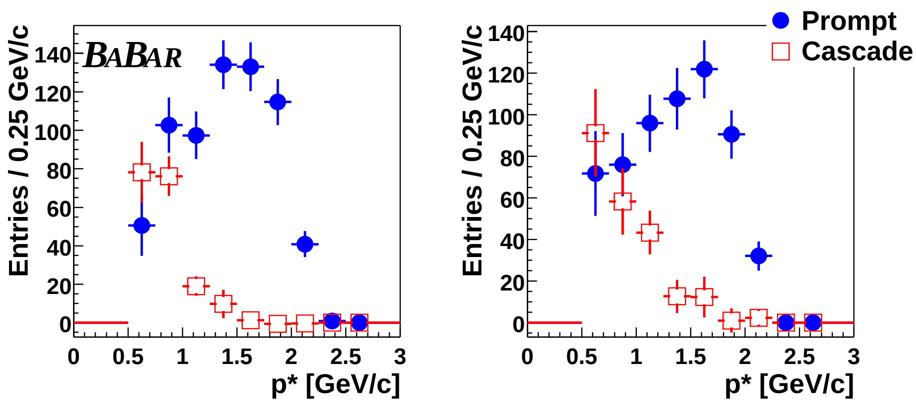

Figure 3: Momentum spectra for prompt and cascade electrons in events tagged with fully reconstructed $B^{\pm}$ (at left) and $B^0/\bar{B}^0$ decays (at right).

3 Inclusive $\mathcal{B}(B \to Xe\nu)$ tagged with leptons

An alternative to the method described in section 2 is to tag the B flavor with a high momentum electron. Non-$B\bar{B}$ events are suppressed by requiring the second Fox-Wolfram moment to be smaller than 0.6 and at least four charged particles within the EMC acceptance. If four charged tracks are present, at least two energy deposits in the calorimeter not associated with the tracks are required in addition. Electrons are selected using the likelihood based algorithm. A minimum center-of-mass momentum p^* of 0.5 GeV$/c$ helps reduce background electrons from sources like photon conversions. Electrons which have not been identified as part of a photon conversion, Dalitz or J/ψ decay are considered as tag if $p^* > 1.4\,\mathrm{GeV}/c$. The preliminary results quoted below are based on 4.1 fb^{-1} and 0.97 fb^{-1} of data recorded on and 40 MeV below the $\Upsilon(4S)$ resonance.

In contrast to the analysis described in section 2, we observe a background to the right-sign sample that originates from a semileptonic charm particle decay of the form

$$\bar{B} \to X_c e^-_{tag} \bar{\nu}_e, \quad X_c \to Y e^+_{cand} \nu_e.$$

With increasing momentum, candidate electrons produced in these cascades show an increasing back-to-back correlation to the tag lepton (Fig. 4a). On the other hand, since the two B mesons are produced nearly at rest in the $\Upsilon(4S)$ rest frame, right-sign prompt electrons produced via

$$\bar{B} \to X_c e^-_{tag} \bar{\nu}_e, \quad B \to Y_{\bar{c}} e^+_{cand} \nu_e$$

show no angular correlation to the tag (Fig. 4b). Therefore we suppress these same-side cascades by a momentum dependent cut as indicated in Fig. 4.

After correcting for acceptance and efficiency we arrive at $25611 \pm 492_{(stat)}$ prompt electrons, resulting in a branching fraction of

$$\mathcal{B}(B \to Xe\nu) = 10.84 \pm 0.21_{(stat)} \pm 0.34_{(syst)}.$$

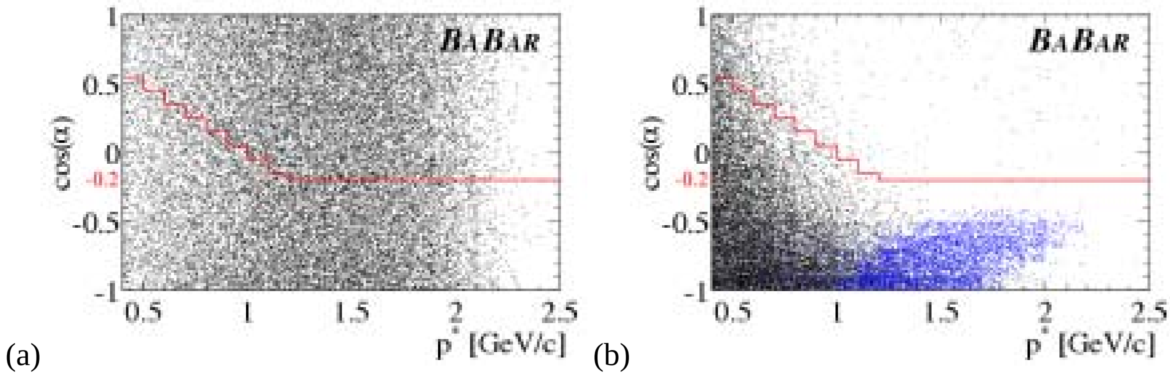

Figure 4: Distribution of angle between tag and candidate electron for prompt (left) and cascade electrons (right). Solid line indicates the cut used to suppress the latter.

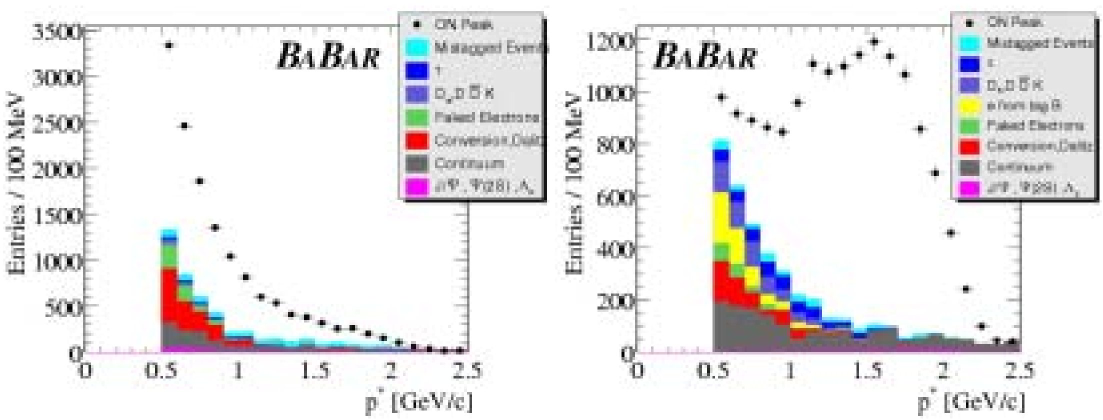

Figure 5: Momentum spectra of right-sign (left) and wrong-sign(right) electrons and backgrounds for lepton tag analysis. Solid points show electron spectra without any background correction applied.

Table 2 breaks down the individual contributions to the systematic error.

One can then exploit the relation [2]

$$|V_{cb}| = 0.0400\eta_{QED}(1 \pm 0.030 \pm 0.024 \pm 0.025 \pm 0.012)\sqrt{\frac{\mathcal{B}(B \to X\ell\nu) - \mathcal{B}(B \to X_u\ell\nu)}{0.105}\frac{1.6\,\mathrm{ps}}{\tau_B}},$$

where $\eta_{QED} = 1.007$, $\tau_B = (1.604 \pm 0.024)\,\mathrm{ps}$, and $\mathcal{B}(B \to X_u\ell\nu) = (1.67 \pm 0.55) \times 10^{-3}$ [7] to obtain

$$|V_{cb}| = 0.0406 \pm 0.0009_{exp} \pm 0.0019_{theor}.$$

Table 2: Contributions to the systematic error of $\mathcal{B}(B \to X_c e\nu)$ tagged with high-momentum electrons.

Source	$\Delta x/x[\%]$	$\Delta\mathcal{B}/\mathcal{B}[\%]$
Electron efficiency	1.3	± 0.155
Continuum subtraction	0	± 0.080
Conversions	13	± 0.065
Dalitz	19	± 0.029
Tracking efficiency	1	± 0.108
Analysis efficiency		± 0.073
N_{tag}	0.64	± 0.069
e in mistagged events	20	± 0.060
e from same B	5	± 0.040
Extrapolation to $p^* = 0$	0.39	± 0.042
Mixing χ_0	6.6	± 0.045
e from D_s^+	45	± 0.192
e from $D\bar{D}K$	25	± 0.101
e from τ	18	± 0.003
e from J/ψ		± 0.077
Total		± 0.337

4 Inclusive $\mathcal{B}(B \to X_u e\nu)$ at the kinematic endpoint

In the rest frame of the B meson, the kinematic endpoint of the electron spectrum for the dominant $B \to X_c e\nu$ decays is at approximately 2.3 GeV$/c$ while that for $B \to X_u e\nu$ decays is at 2.6 GeV$/c$. Even though the spectrum is convoluted by a spread of ± 0.2 GeV$/c$ due to the B meson's average 0.3 GeV$/c$ momentum in the $\Upsilon(4S)$ rest frame, a narrow interval remains that is dominated by electrons from $B \to X_u e\nu$ decays. It covers approximately 10% of the total electron spectrum for charmless semileptonic B decays. The extrapolation from the limited momentum range near the endpoint to the full spectrum is nontrivial since OPE breaks down in this part of phase space. This analysis follows the method used in previous measurements by the ARGUS [3] and CLEO [4, 5] collaborations. The data sample corresponds to an integrated luminosity of 20.6 fb^{-1} collected at the $\Upsilon(4S)$ resonance, and 2.6 fb^{-1} recorded 40 MeV below the resonance.

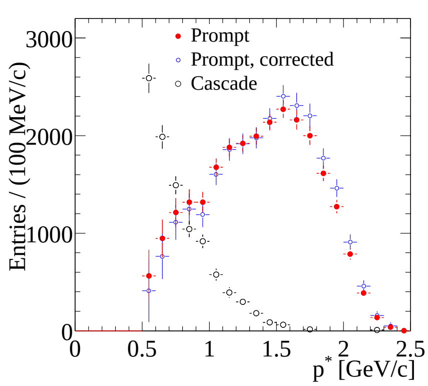

Figure 6: Momentum spectra of prompt and cascade electrons before and after correction for electron identification efficiency.

For this analysis, electron candidates are selected in the momentum range from 1.5 to 3.5 GeV/c in the $\Upsilon(4S)$ rest frame. The solid angle is restricted by the electromagnetic calorimeter coverage, defined by the laboratory polar angle range of $-0.72 < \cos\theta_{lab} < 0.92$. In this momentum and angular range, the efficiency for identifying an electron has meen measured to be $\varepsilon_{PID} = 0.91 \pm 0.02$, the average hadron misidentification probability is less than 0.2%. To suppress low-multiplicity QED processes, including $\tau^+\tau^-$ pairs, the number of charged tracks per event is required to be greater than three. This background and non-resonant hadronic events are further suppressed by a restriction on the ratio of Fox-Wolfram moments $H_2/H_0 < 0.4$.

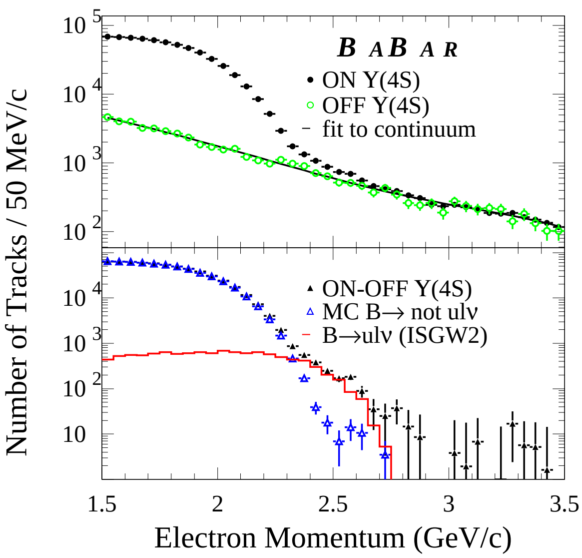

Figure 7: Electron momentum spectrum in the $\Upsilon(4S)$ rest frame. The upper plot shows on-peak data and off-peak data scaled to the on/off-peak ratio. In the lower plot the continuum has been subtracted from on-peak data. In addition the Monte Carlo predictions for $B\bar{B}$ background (open triangles) and $B \to X_u e\nu$ (solid line) are indicated.

Table 3: Electron yields for $\mathcal{B}(B \to X_u e\nu)$ at the kinematic endpoint. N_{ON} is the number of selected electrons recorded on the $\Upsilon(4S)$ resonance, N_{OFF} is the fitted number of continuum background events. The other contributions are estimated from Monte Carlo simulations.

p^* [GeV/c]	2.0–2.3	2.3–2.6
N_{ON}	74140±272	6455±80
N_{OFF}	7749±165	4051±93
$N_{b\to c\ell\nu}$	61158±470	470±41
N_{BG}	1377±71	238±31
$N_{b\to u\ell\nu}$	3857±572	1696±133

The raw spectrum of the highest momentum electron in events satisfying the described criteria is shown in Figure 7, along with the nonresonant background contribution. The number of selected events, split into two momentum intervals, are listed in Table 3.

The fully corrected differential branching ratio as a function of the electron momentum is presented in Figure 8. The partial branching fraction $\Delta\mathcal{B} = (N_{ON} - N_{OFF} - N_{b\to c\ell\nu})(1/2\varepsilon N_{B\bar{B}})(1+\delta_{rad})$ is obtained from integrating over the interval $2.3 < p^* < 2.6\,\mathrm{GeV}/c$:

$$\Delta\mathcal{B}(B \to X_u e\nu) = (0.152 \pm 0.014_{(stat)} \pm 0.014_{(syst)}) \times 10^{-3}.$$

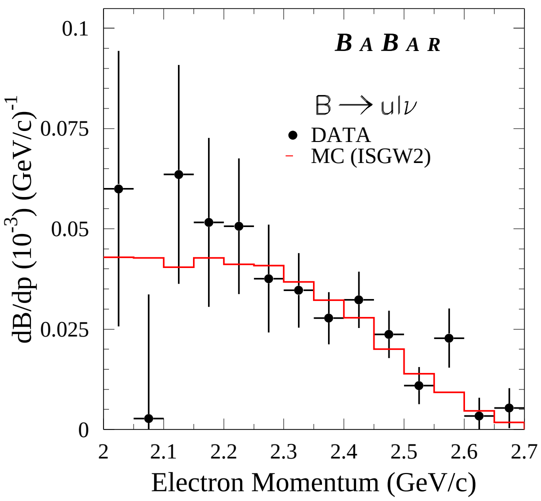

Figure 8: The branching ratio $\mathcal{B}(B \to X_u e\nu)$ as a function of electron momentum in the $\Upsilon(4S)$ rest frame. The data (statistical errors only) are compared to a prediction based on the ISGW2 model [6] assuming a total inclusive branching ratio of 10^{-3} for $B \to X_u e\nu$ decays of with X_u masses up to 1.5 GeV/c^2.

Table 4: Contributions to the systematic error of $\mathcal{B}(B \to X_u e\nu)$ measured at the kinematic endpoint.

Source	$\Delta x/x$	$\Delta\mathcal{B}/\mathcal{B}$
Efficiency	5	5
Continuum subtraction	2	5
Background $b \to c\ell\nu$	4	1
Background $B \to J/\psi(\to e^+e^-)X$	20	1
Background $B \to X_c$ misidentified	28	2
B movement	5	5
$N_{B\bar{B}}$	2	2
Radiative corrections	10	1
Total		9

This result agrees very well with the measurement by the CLEO collaboration [5] Individual contributions to the systematic error are detailed in Table 4.

The charmless semileptonic branching fraction $\mathcal{B}(B \to X_u e\nu)$ can be extrapolated from the partial branching fraction $\Delta\mathcal{B}$ using Heavy Quark Theory, which describes the Fermi motion of the quarks inside the meson in terms of a shape function. To leading order, the same shape function describes all $b \to q\ell\nu$ transitions, where q is any light quark. The CLEO collaboration [8] has recently used the measurement of the inclusive photon spectrum from $b \to s\gamma$ transitions to derive the parameters describing the shape function. Using their measurement for the interval $2.3 < p^* < 2.6\,\mathrm{GeV}/c$, we extrapolate our result to the total branching ratio and make use of the relation [9]

$$|V_{ub}| = 0.00445\sqrt{\frac{\mathcal{B}(B \to X_u\ell\nu)}{0.002}\frac{1.55\,\mathrm{ps}}{\tau_B}}(1.0 \pm 0.020 \pm 0.052)$$

to arrive at our preliminary result for $|V_{ub}|$:

$$|V_{ub}| = (4.43 \pm 0.29_{exp} \pm 0.25_{OPE} \pm 0.50_{f_u} \pm 0.35_{s\gamma}) \times 10^{-3}.$$

5 Conclusion

We have presented preliminary results for inclusive branching fractions of $B \to X_c e\nu$ and $B \to X_u e\nu$, and used these to calculate $|V_{cb}|$ and $|V_{ub}|$. All of them are based on samples representing 20% or less of the *BABAR* data recorded to date. The statistics are therefore expected to improve considerably in the future. In addition, inclusive $|V_{ub}|$ analysis, measurements of the $b \to s\gamma$ photon spectrum, and extraction of $|V_{cb}|$ from hadronic mass moments are in progress.

References

[1] B. Aubert *et al.*, The *BABAR* detector, Nucl. Instr. and Methods A **479**, 1 (2002).

[2] I. Bigi *et al.*, Ann. Rev. Nucl. Part. Sci. **47**, 591 (1997); Bagan *et al.*, Phys. Lett. B **342**, 362 (1995).

[3] The ARGUS Collaboration, H. Albrecht *et al.*, Phys. Lett. B **234**, 409 (1990) and Phys. Lett. B **255**, 297 (1991).

[4] The CLEO Collaboration, R. Fulton *et al.*, Phys. Rev. Lett. **64**, 16 (1990)

[5] The CLEO Collaboration, F. Bartelt et al., Phys. Rev. Lett. **71**, 4111 (1993).

[6] N .Isgur *et al.*, Phys. Rev. D **39**, 799 (1989); D. Scora *et al.*, Phys. Rev. D **52**, 2783 (1995).

[7] D.E. Groom *et al.*, Eur. Phys. Jour. C **15**, 1 (2000).

[8] The CLEO Collaboration, hep-ex/020219.

[9] I. Bigi, hep-ph/9907270, revised at 2002 CKM Workshop.